International Journal of Scientific Engineering and Science
Volume 2, Issue 11, pp. 65-70, 2018. ISSN (Online): 2456-7361

Investigation of Static Structure Effect According to Axial Coordinates by Using Finite Element Method in Ansys Workbench Software of AISI 310 Austenitic Stainless Cylindrical Model Steel

Semih Taskaya[1*], Selim Taskaya[2]
[1]Department Metallurgy and Materials Engineering, Firat University, Elazig, Turkey-23119
[2]Department Architecture and Urban Planning, Artvin Coruh University, Artvin, Turkey-08100
E-mail: muh.semihtaskaya@gmail.com, selim_taskaya@artvin.edu.tr
*Corresponding author: muh.semihtaskaya@gmail.com

***Abstract*—** *AISI 310 quality austenitic stainless steel, C ratio less than 0.25, is one of the most widely used and most durable steels designed for industrial applications. Finite element method (FEM) is a metric that provides the solution of complex engineering problems with controllable parts that can be reduced by the base. Applied in this study, 40 mm outer diameter, AISI 310 stainless steel cylinder containing mechanical properties are modeled in Ansys Workbench 12.0 module. The design is performed by fixing the cylindrical steel from the substrate support zone. The static structural solution of the steel was analyzed by applying a force of 1000 N in the -y-axis direction from the steel top plate zone. In Ansys software, deformation deformation of cylindrical steel, simulating solution in Workbench module and finite element method, max.- min. stress and elastic stresses, and vectorial component analyzes. As a result of the analyzes, it was observed that the charge distributions effected by the static structure of the cylindrical steel were concentrated in the upper and lower regions.*

***Keywords*—** *AISI 310, Ansys Workbench, Finite element method, Static structure.*

I. INTRODUCTION

Processed austenitic stainless steel alloys are widely used in many applications including biomedical, petrochemical and high temperature applications [1-8]. They show the perfect combination of corrosion resistance, weldability, phase stability and formability. Stainless steel grade AISI 310 is one of the most widely used steels for industrial applications. In the absence of sulfur in the working environment, it can be used at temperatures up to 1150 °C. Similar to other austenitic steel grades, the alloy AISI 310 has excellent mechanical properties and high temperature stability. Alloy; high temperature properties thanks to its high chromium content. Chromium can also improve the corrosion and oxidation resistance of the alloy. This alloy is not only resistant to high temperature oxidizing environments, but also has good resistance to carburizing environments. These features and high creep resistance make the AISI 310 steel a typical choice for heat exchangers and furnace tubes. Components used in high temperature applications normally fail for a variety of reasons; creep [2], microstructural degradation [3,4], thermal fatigue [5-7], carburization and graphitization [8], erosion-corrosion and sigma-phase embrittlement [9-19]. Secondly, it is mostly due to a phase transformation observed when the components remain at high temperatures. The formation of the ir-phase adversely affects the mechanical properties of alloys as well as corrosion [12-13]. In the context of metal cutting, a large tension, large tension ratio and high temperature are generally reported in the literature. It is well known that the microscopic and macroscopic response of the material under high stress-rate loads is influenced by the tensile, stretching rate, temperature and microstructure of the material. Therefore, in order to accurately analyze this process using numerical methods such as the finite element method (FEM), the material constructing behavior information under these severe loading conditions is a prerequisite and therefore the correct workflow flow stress data should be used. In fact, the success and reliability of digital models depends mainly on the properties of mechanical (elastic constants, flow stresses, fracture stress / strain, etc.) and thermo-physical (density, thermal conductivity, heat capacity, etc.). The correct selection of these parameters, such as the material and contact conditions in tool-chip and tool-work interface interfaces [14-18], the accuracy of one person, temperatures, chip morphology, tool wear and the surface integrity of the finished parts as a result (residual stresses, surface roughness, microstructure, etc.). Although many studies on the finite element (FEM) modeling of orthogonal cutting have been published, recent reviews [19,20] have shown that they mainly focus on stresses, stress and shear temperatures. In the literature, only a few studies can be found on FEM modeling, including the prediction of processing residual stresses, with special attention to residual stresses in flat carbon steels and hardened steels [19-22]. In his study, Taskaya in the Ansys program of St 37 steel, with the finite element method (FEM), investigated the degree of increase in the effect of mechanical stress distributions on the supports according to the pressure in the simulation analysis [23]. In his study, Taskaya investigated the deformation, mechanical and elastic stress analysis of the beam axes by applying different load and constant pressure to the 3D lattice roof model with an isotropic steel material by using finite element method (FEM) [24]. Gür et al. designed an isotropic steel material as a 3-dimensional lattice roof and investigated the effects of mechanical stress on beam axes

with respect to different loads according to the finite element method (FEM) [25]. In their study, Gür et al. examined the stress analysis in the different supports and geometries of the sandwich composite by using the finite element method and compared the changes in the material [26]. Taskaya et al., in their work, according to the finite element method (FEM) in the Ansys software, St 70 roof cage steel according to the St 37 roof cage steel, the axis of the axes of both forces and moments of deformation and observed that the increase in the stress of the vector [27]. Kaymaz et al., in the study, consisting of 3 intermediate layers, 7 degree orientation angle with 2 different radial geometry geometry model, x, y, z coordinate dimensions according to the Ansys software in 3-dimensional FEM method. In two different tests, the flat and radial geometry sandwich plates were fixed by linear and linear fixation from the right and left supports, and they performed mechanical stress analysis at 4 MPa under axial pressure. Geometric shapes of the same-bearing different and geometric shapes of different-bearing comparing the same structures have examined [28]. Polat et al. studied the finite element method (FEM) analysis of the functionally graded continuous contact problem, which was seated with elastic semi-infinite plane and loaded with rigid two blocks [29]. Polat et al. investigated the comparative analysis of the problem of continuous contact in a homogeneous layer, which was seated in an elastic semi-infinite plane and loaded with rigid two blocks [30].

In this study, the main purpose of using Ansys software with finite element method is to pre-check the simulation studies without going to the application stage of mechanical improvements according to the parameters determined on steel structures.

II. MATERIALS AND METHODS

A. Modeling of AISI 310 Cylindrical Steel

In the Ansys 12.0 software, in the Workbench interface module, the mechanical properties of the AISI 310 stainless cylindrical model steel indicated by Table I are defined in the Ansys Workbench data library and the Workbench design module is configured to create the geometry of the model.

TABLE I. Mechanical properties of AISI 310 stainless steel [31].

Material	Density (d), (kg/m^3)	Modulus of Elasticity (E), (MPa)	Elongation (€), (%)	Poisson Ratio (υ)	Tensile strength (σ_c), (MPa)	Yield strength (σ_a) (MPa)	Fatigue Life (N), (N/mm$^{2)}$
AISI 310	7750	200000	40	0.3	515	205	95

In the design section, the cylindrical steel model is formed as seen in Fig. 1a in the cylindrical circle position of 40 mm diameter. The circle is given a length of 40 mm relative to the z axis and the base region of the circle is modeled by cloning according to the -z axis of the same length. The model is transformed into a solid model with the steel structure generate module (Fig. 1b-c).

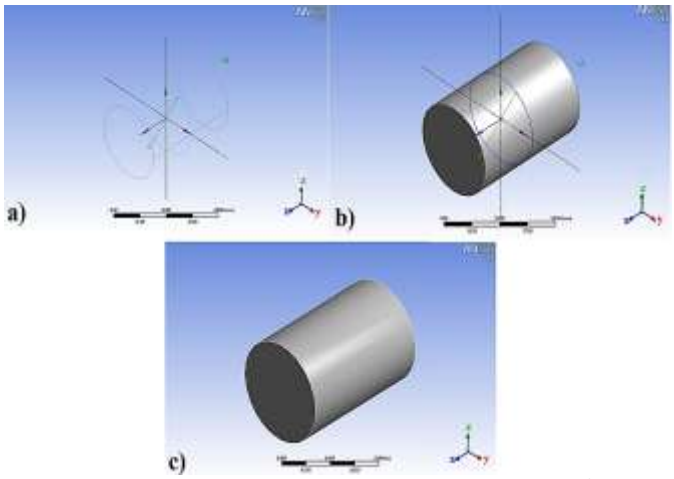

Fig. 1. Cylindrical steel Ansys Workbench modules a) linear circle formation b) solid model transformation c) solid model view

B. Meshing of AISI 310 Cylindrical Steel (Network layer) Operation

AISI 310 cylindrical steel model, structure model to simulate the mechanical properties of a mesh layer is defined. A uniform web layer is formed as shown in Fig. 2 at the workbench interface.

C. AISI 310 Cylindrical Steel Fixing and Load Application

In Ansys Workbench software, as the next step after the mesh process, AISI 310 cylindrical steel as shown in Fig. 3 is selected by applying the substrate region of the model. The regional axis in the upper layer of the fixed steel structure, ie the regional field marked by red in Fig. 3b, is modeled by creating a compression effect at the force of 1000 N on the –y axis.

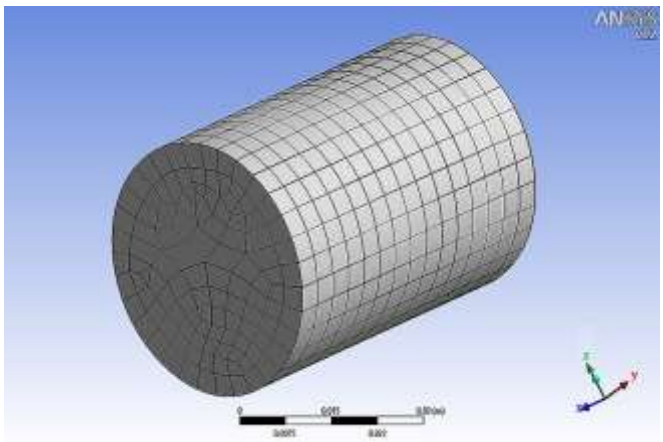

Fig. 2. Meshing of cylindrical steel in Ansys Workbench module

The main purpose of the meshing process is to provide the mechanical and physical properties of the material to be contacted by the transitions in the web layer and the interactions are simulated as a spring wave. These simulations result in the analysis by measuring the response to the load in the model. Meshing in Ansys software, the modeled axis is defined as narrower spacing in order to obtain efficiency from

Volume 2, Issue 11, pp. 65-70, 2018. ISSN (Online): 2456-7361

the analysis results in the model examined, while the entire model is defined as a fixed min. value is formed in the range of automatic mesh.

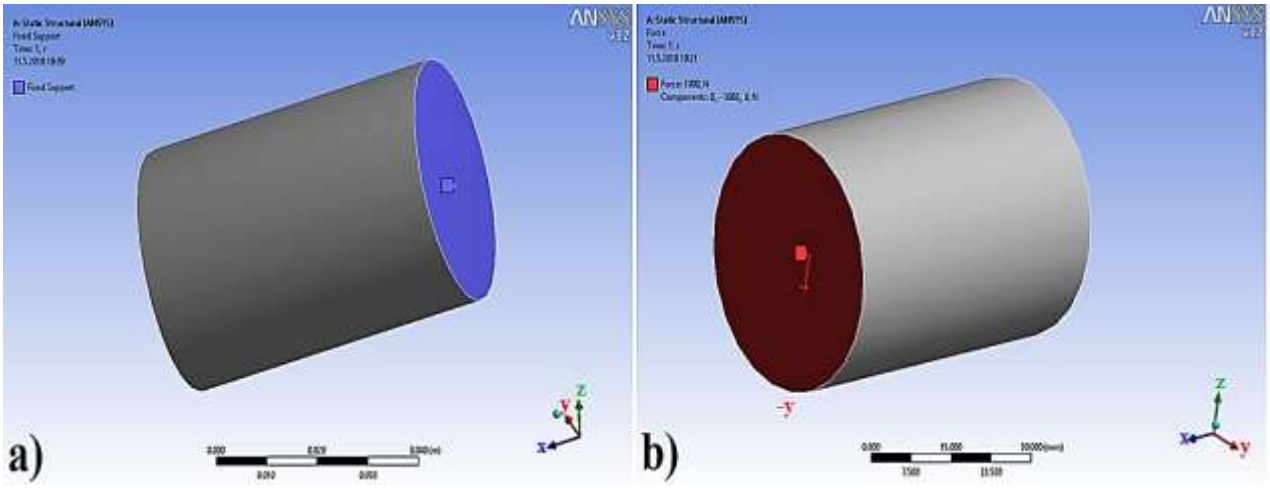

Fig. 3. Cylindrical steel Ansys Workbench modules a) fixing from the subbase b) applying force on the -y axis

III. RESULTS AND DISCUSSION

Steel model structure is solved with the solve module and the static structure analysis of the model is completed. Static structure findings of the steel model, deformation shape changes, vector composite analysis, max.-min elastic stresses between equivalent surfaces, equivalent and principal stress points of the knots were examined.

The deformation shape changes according to the load applied on the -y axis of the steel cylinder specified in Fig. 4 were examined. The contour simulation shown in Fig. 4a shows the total amount of deformation that the steel structure shows from the applied load region to the fixed support region. Here, when the scale result is compared, the deformation per mesh unit is measured as 0.0038 mm max. a spring wave equal to the point-z symmetry axis. Deformation progression is distributed in equal position with approximately 0.0005 mm mesh spacing. In Fig. 4b, the directed leaf position of the deformation shape is simulated. The directional deformation here is taken over the x-axis. When the results of the analysis are taken into consideration, the red regions at the middle nodes of the deformations have a draw effect with $9.85x10^{-5}$ mm distances, and when the color distribution with the distances about $2x10^{-5}$ mm is touched in blue, it has produced a pressing effect on the side axes of the steel structure according to the load. These stresses have an inward effect on the side knot axes as well as creating residual stresses in the upper and lower areas of the load distance.

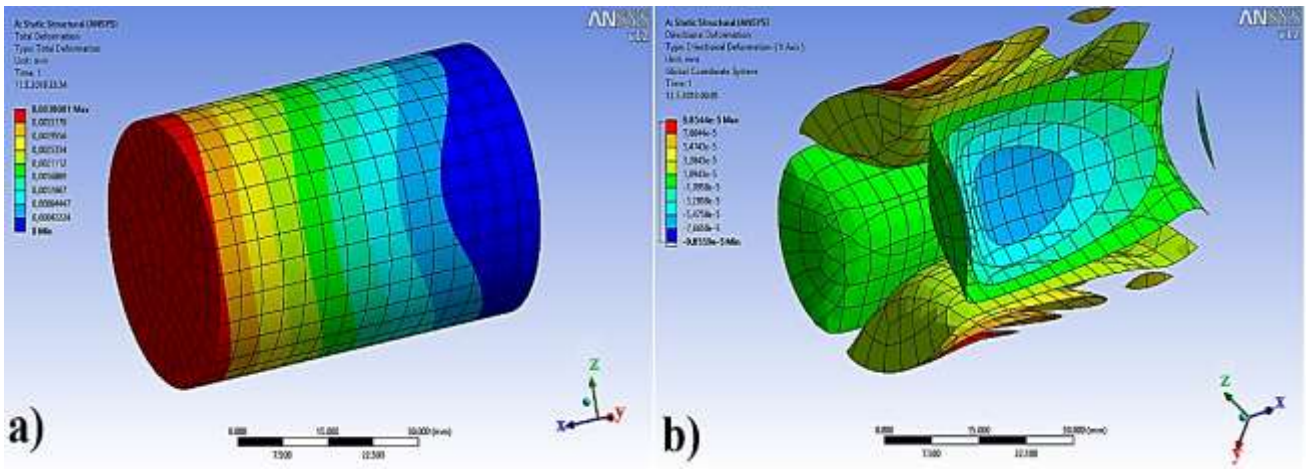

Fig. 4. Cylindrical steel Ansys Workbench modules a) Total deformation simulated analysis b) Directed surface analysis of the deformation shape

In Fig. 5, the distribution rate of the static structure shown in the model is examined as vectoral composition. When the load is applied in Fig. 5a, the vector components move relative to the -z axis as the load continues from the axis -y. As shown in Fig. 5b, the rate of propagation increases as the vector component load simulation distribution accelerates.

Volume 2, Issue 11, pp. 65-70, 2018. ISSN (Online): 2456-7361

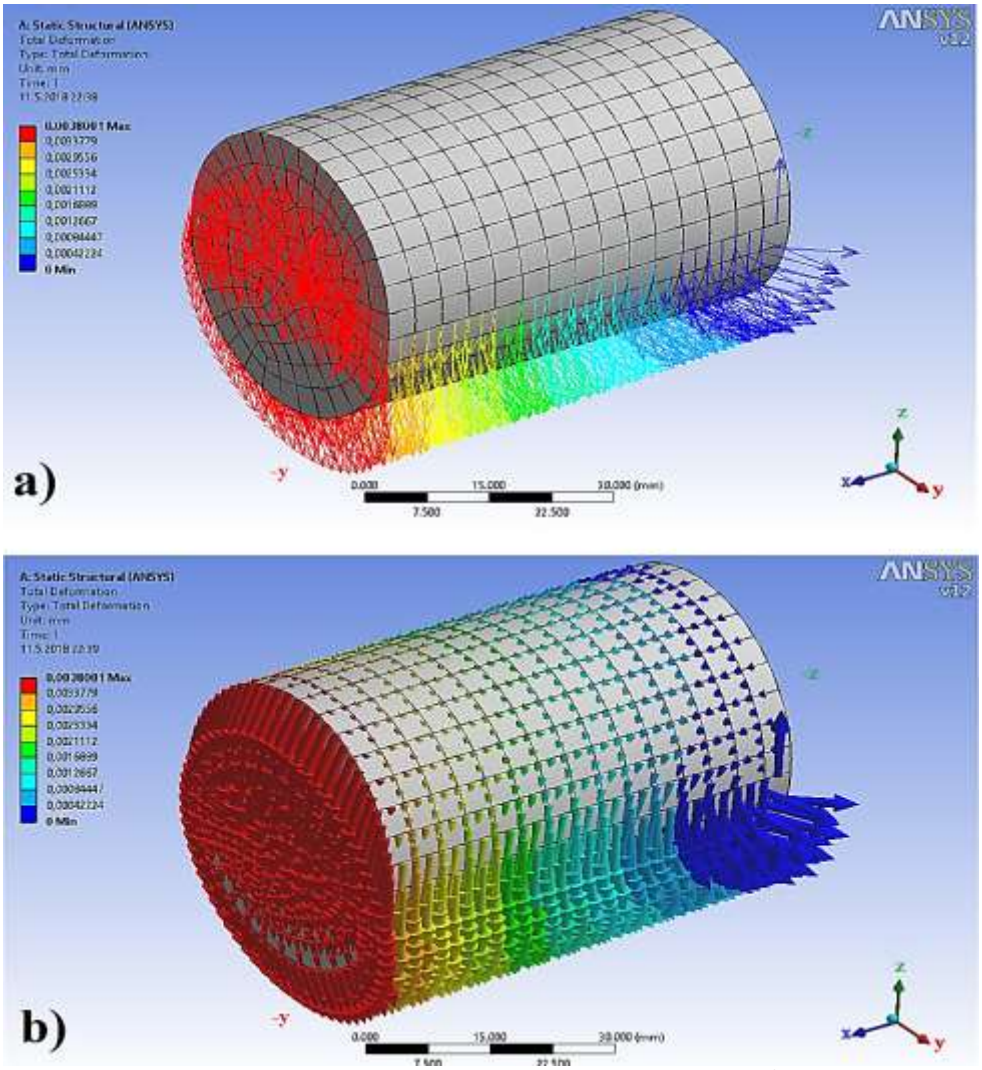

Fig. 5. Cylindrical steel Ansys Workbench modules a) vectorial composition b) simulation of vector composite analysis

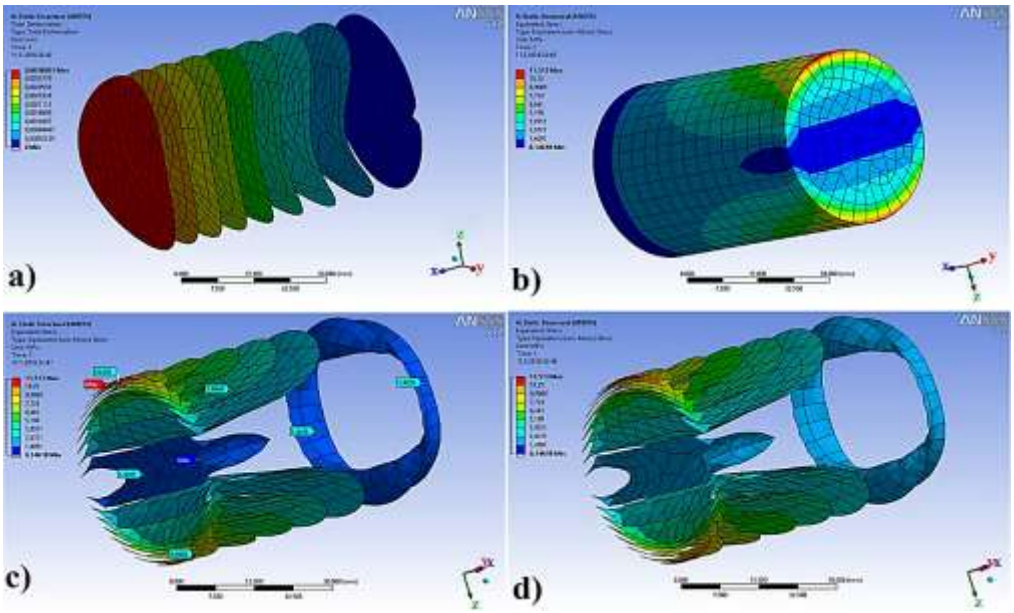

Fig. 6. Cylindrical steel Ansys Workbench modules a) leaf modulus representation of deformation between coaxial surfaces b) equivalent von mises voltage c) equivalent von mises voltage max.-min. and the stresses at the designated nodes d) the leaf module of the von mises voltage between the coherent surfaces

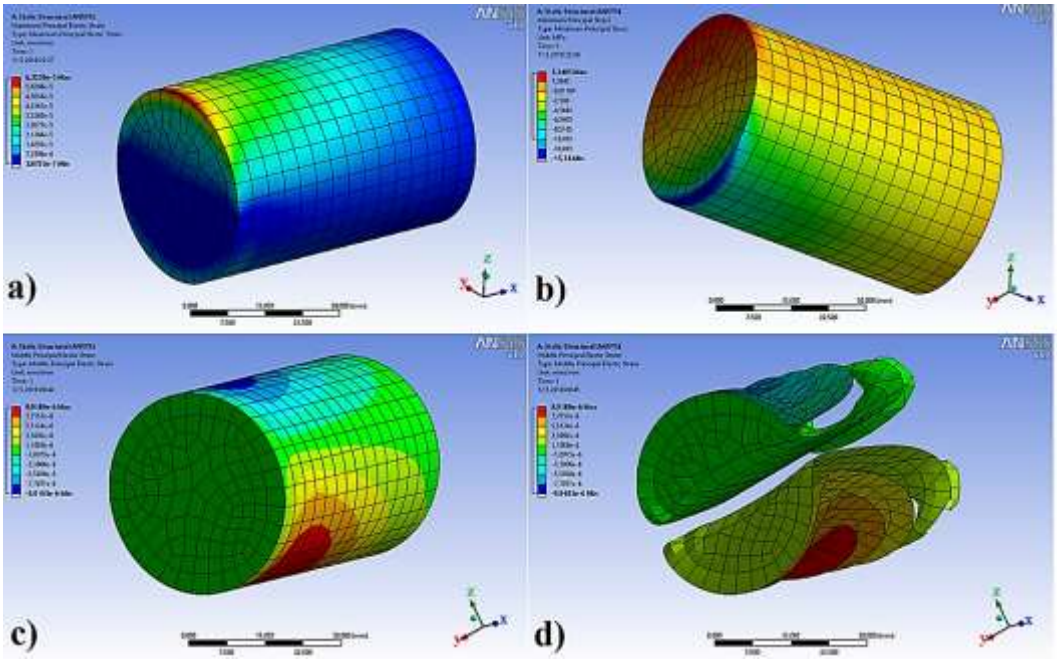

Fig. 7. Cylindrical steel Ansys Workbench modules a) max. elastic stress in the region b) min. c) the elastic stress in the core region c) the elastic modulus in the central region of the knot

IV. Conclusions and Recommendations

The following results were observed when Aisi 310 austenitic stainless steel model was applied to the Ansys software with force effect press.

- The leaf module of the deformation shape between the equal surfaces gives the results of the simulation distributions in the Ansys software as a spring wave between the axes.
- The von mises stress on the coherent surfaces which are the average value of the stresses and shear stresses on the steel cylindrical model were investigated.
- Given the contour simulated test result of the shear stresses, the red max. stress node regions are concentrated in the upper and lower axis base regions. These intensified nodes were observed to be subjected to a tension of about 11.50 MPa. More detailed description of this result In Fig. 6c, the max.-min. points of the steel structure and the stresses in the determined nodes were tested. Red zone max. from the stress point, min. load reduction simulations were observed towards the stress blue areas.
- The elastic tension of the main region at the max. point of the static steel structure in Fig. 7a is determined. The max. node at the $6.32x10^{-5}$ mm distance point is the point at which the most elastic stress occurs. It is observed that the elastic tension in the direction of the distances of $1.5x10^{-5}$ mm, and the distribution in the upper base area of the distribution in the whole model.
- In Fig. 7b, the tension of the steel structure in the min. main zone was investigated. The min. point where the tension creates a pressing effect is the bottom base region, which is the point of touch in the model. It was analyzed that the test result produced a compression effect of 15.74 MPa.
- In Figs. 7c-d, the elastic behavior of the middle nodes in the main region was tested. At a distance of $9.91x10^{-6}$ mm max. mesh, a tensile effect was observed in the lower knot at the middle knot regions of the model at intervals of about $2x10^{-6}$ mm, and a pressing effect was observed in the upper base as seen in the leaf modules more comfortable.

From this model test results, the steel model structure from constructive aspect yielded the expected positive results from the different modules in Ansys Workbench software. All results from the model can be tested for all stresses from different regional axes. Model measurements, mesh structure, load amount, fixing angle and direction, complex model structures, changes in the type of analysis can be compared by changing the structure. Different simulation tests can be carried out using different finite element software (such as Apex, Nastran, Patran) [24]. As a result of the data obtained in this study, AISI 310 austenitic stainless steel model's Ansys Wokbench software, determined in the regional axes and force deviation of the angle of deflection, nodes, deformation changes and stresses, load-dependent changes in load due to a change in the pressure is determined from the tests. With this kind of finite element software, it is aimed to determine what kind of effect of a mechanical change without applying to the application stage, in the direction of mechanical improvements model type, changing parameters and applying different kind of test analysis to get the best results.

References

[1] H. Lavvafi, M. E. Lewandowski, D. Schwam, and J. J. Lewandowski, "Effects of surface laser treatments on microstructure, tension, and fatigue behavior of AISI 316LVM biomedical wires," *Mater. Sci. Eng. A*, vol. 688, issue 14, pp. 101-113, 2017.

[2] R. A. Kumar, S. K. Sinha, Y. N. Tiwari, J. Swaminathan, G. Das, and S. Chaudhuri, "Analysis of failed reformer tubes," *Eng. Fail. Anal.*, vol. 10, pp. 351-358, 2003.

[3] N. Ejaz and A. Tauqir, "Failure due to structural degradation in turbine blades," *Eng. Fail. Anal.*, vol. 13, pp. 452-463, 2006.

[4] C. Barbosa, J. L. Nascimento, I. M. V. Caminha, and I. C. Abud, "Microstructural aspects of the failure analysis of nickel base superalloys components," *Eng. Fail. Anal.*, vol. 12, pp. 348-361, 2005.
[5] H. T. Pang and P. A. S. Reed, "Microstructure effects on high temperature fatigue crack initiation and short crack growth in turbine disc nickel-base superalloy Udimet 720Li," *Mater. Sci. Eng. A*, vol. 448, pp. 67-79, 2007.
[6] O. Coreño-Alonso, A. Duffus-Scott, C. Zánchez-Cornejo, J. Coreño-Alonso, F. Sánchez-de Jesús, and A. Bolarín-Miró, "On the effect of σ-phase formation during metal dusting," *Mater. Chem. Phys.*, vol. 84, pp. 20-28, 2004.
[7] K. Kobayashi, K. Yamaguchi, M. Hayakawa, and M. Kimura, "Grain size effect on high-temperature fatigue properties of alloy718," *Mater. Lett.*, vol. 59, pp. 383-386, 2005.
[8] S. A. J. Jahromi, S. Javadpour, and Kh. Gheisari, "Failure analysis of welded joints in a power plant exhaust flue," *Eng. Fail. Anal*., vol. 13, pp. 527-536, 2006.
[9] A. V. Kington and F. W. Noble, "σ phase embrittlement of a type 310 stainless steel," *Mater. Sci. Eng. A*, vol. 138, pp. 259-266, 1991.
[10] J. Barcik, "The kinetics of σ-phase precipitation in AISI310 and AISI316 steels Metall," *Mater. Trans. A*, vol. 14, pp. 635-641, 1983.
[11] H. D. Solomon, TM. Devine, and R. D. Lula (Ed.), "Duplex Stainless Steels," *American Society for Metals. Metals Park, OH*, pp. 693-756, 1983.
[12] H. M. Ezuber, A. El-Houd, and F. El-Shawesh, "Effects of sigma phase precipitation on seawater pitting of duplex stainless steel," *Desalination*, vol. 207, pp. 268-275, 2007.
[13] N. Lopez, N. Cid, and M. Puiggali, "Influence of σ-phase on mechanical properties and corrosion resistance of duplex stainless steels," *Corros. Sci.*, vol. 41, pp. 1615-1631, 1999.
[14] T.H.C. Childs, "Material property needs in modelling metal machining, in: Proceedings of the CIRP," *International Workshop on Modeling of Machining Operations, Atlanta, Georgia*, pp. 193–202, 1998.
[15] E. M. Trent, "Wrigth P.K. Metal Cutting (fourth ed.)," Butterworth-Heinemann, Stoneham, MA, p. 434, 2000.
[16] M. C. Shaw, "Metal Cutting Principles (second ed.)," Oxford Science Publications, Oxford, p. 651, 2005.
[17] T. H. C. Childs, K. Maekawa, T. Obinakawa, and Y. Yamane, "Metal Machining," Theory and Applications Elsevier, Amsterdam, p. 408, 2000.
[18] V. P. Astakhov, "Metal Cutting Mechanics," CRC Press. Boca Raton, FL, pp. 297, 1999.
[19] J. Mackerle, "Finite-element analysis and simulation of machining: a bibliography (1976–1996)," *Journal of Materials Processing and Technology*, vol. 86, issue (1–3), pp. 17-44, 1999.
[20] J. Mackerle, "Finite element analysis and simulation of machining: an Addendum A bibliography (1996–2002)," *International Journal of Machine Tools & Manufacture*, vol. 43, pp. 103-114, 2003.
[21] R. M'Saoubi, J.C. Outeiro, B, Changeux, J. L. Lebrun, and A. M. Dias, "Residual stress analysis in orthogonal machining of standard and resulfurized AISI 316L steels," *Journal of Materials Processing and Technology*, vol. 96, issue (1–3), pp. 225-233, 1999.
[22] J.C. Outeiro, A.M. Dias, J.L. Lebrun, and V. P. Astakhov, "Machining residual stresses in AISI 316L steel and their correlation with the cutting parameters," *Machining Science and Technology*, vol. 6 issue 2, pp. 251-270, 2002.
[23] S. Taşkaya, "St 37 çeliğinin Ansys programında basınca bağlı olarak mekanik gerilmelerin incelenmesi," *The Journal of International Manufacturing and Production Technologies (JIMPOT)*, vol. 1, issue 1, pp. 39-46, 2017.
[24] S. Taşkaya, "Investigation of mechanical and elastic stresses in ansys program by finite elements method of 3D lattice roof model," *Mugla Journal of Science and Technology*, vol. 4, issue 1, pp. 27-36, 2018.
[25] A. K. Gür, S. Taskaya, N. Kati, and T. Yildiz, "Investigation of mechanical stresses of 3d truss roof model by ansys method," *2nd International Conference on Material Science and Technology in Cappadocia (IMSTEC'17)*, Nevşehir, pp. 11-15, 2017.
[26] A. K. Gür, S. Taskaya, N. Kati, and T.Yildiz, "Investigation of stress analysis in sandwich composite plates by Ansys method," *8th International Advanced Technologies Symposium (IATS'17)*, Elazığ, pp. 495-509, 2017.
[27] S. Taşkaya, B. Zengin and K. Kaymaz, "Investigation of force and moment effect of St 37 and St 70 roof lattice steels in Ansys program," *Middle East Journal of Science*, vol. 4, issue 1, pp. 23-35, 2018.
[28] K. Kaymaz, B. Zengin, and M. Aşkın ve S. Taşkaya, "Sandviç kompozit tabakalarında mekanik gerilmelerin basınca bağlı olarak Ansys yazılımı ile incelenmesi," *Gümüşhane Üniversitesi Fen Bilimleri Enstitüsü Dergisi, (CMES 2018 Sempozyum Ek sayısı),* pp. 79-93, 2018.
[29] A. Polat, Y. Kaya ve T. Ş. Özşahin, "Fonksiyonel derecelendirilmiş tabakada sürekli temas probleminin sonlu elemanlar yöntemi ile analizi," *20. Ulusal Mekanik Kongresi*, Uludağ Üniversitesi, Bursa, pp. 332-341, 2017.
[30] A. Polat, Y. Kaya ve T. Ş. Özşahin, "Elastik yarı sonsuz düzlem üzerine oturan ağırlıklı tabakanın sonlu elemanlar yöntemi kullanılarak sürtünmesiz temas problemi analizi," *Düzce Üniversitesi Bilim ve Teknoloji Dergisi*, vol. 6, issue 2, pp. 357-368, 2018.
[31] "Steel Eagle Commerce Ltd.," www.steeleaglemalta.com